

## CATASTROPHES IN SURFACE SCATTERING

T.C.M. HORN; A.D. TENNER; PAN HAO CHANG AND A.W. KLEYN

FOM-Institute for Atomic and Molecular Physics, Kruislaan 407, 1098 SJ Amsterdam (The Netherlands).

### ABSTRACT

Simulations to fit a model potential for rainbow scattering of K-ions on W(110) generate a complicated 3-dimensional hypersurface, which is projected onto a detector plane in experiments. To describe those projections catastrophe theory can be applied. To investigate how this theory can be applied some calculations on hard wall scattering have been performed.

### INTRODUCTION

Rainbow scattering of atoms or ions from solid surfaces is a well-known phenomenon. It gives information about the collision dynamics and hence about the interaction potential between projectile and solid. The rainbows appear in the scattered intensity versus the scattering angle. More complicated rainbows can be observed when the scattered intensity is measured as a function of both the scattering angle and the energy transfer to the solid. The latter experiments we have performed for the system  $K^+ + W(110)$  at energies around 35 eV and normal incidence [1]. The data indicate that there is a strong azimuthal dependence of the intensity, leading to so-called "real" rainbows of the triple differential cross section. The experiments can be reproduced successfully using classical trajectory calculations with a realistic interaction potential [2].

Rainbows are examples of elementary catastrophes in catastrophe theory [3]. Catastrophe theory is a mathematical tool to categorize singularities arising from the mapping of more-dimensional continuous hypersurfaces. The presence of elementary catastrophes in light and surface scattering has been demonstrated by M. Berry [4]. In his calculations the Kirchoff's diffraction model has been applied to hard wall scattering. In this article we will perform similar hard wall calculations using simple classical dynamics to clarify the structures observed. The advantage of classical calculations is that the caustics are not masked by diffractive oscillations. With the help of these simple calculations and with scattering calculations on overlapping hard spheres we try to learn how to classify the catastrophes in our realistic simulation. This classification is a direct characterization of the topology of the interaction potential of the system involved. Hopefully these investigations will lead to a new method for

fast determination of important features of gas-surface interaction potentials and, e.g. adsorbate induced, changes thereof.

#### CATASTROPHES IN HARD WALL SCATTERING

To investigate the meaning of catastrophes occurring in surface scattering, some calculations on reflection of particles normally incident on hard surfaces with sinusoidal corrugation have been made. It allows the use of simple geometry to characterize the parameters involved. The two scattering angles, i.e. the polar angle  $\theta$  and azimuthal angle  $\phi$ , are determined by the reflection from the surface and can be written with the hard wall function  $z=f(x,y)$  by the following mapping:

$$\cos\left(\frac{\theta}{2}\right) = (f_x^2 + f_y^2 + 1)^{-\frac{1}{2}} \quad (1a)$$

$$\tan(\phi) = \frac{f_y}{f_x} \quad (1b)$$

Here  $f_x = \partial f / \partial x$  and  $(x,y,z)$  form a usual cartesian coordinate system. The caustics, i.e. the intensity maxima, present in the scattering profile are caused by reflection from certain sets of points in the unit cell. A formula to describe those sets can be derived by considering the points  $(x,y)$  on the surface where one of the two angles  $\theta$  and  $\phi$  is stationary. This leads to the following demand upon the Hessian of the surface function:

$$H[f(x,y)] = f_{xx}f_{yy} - f_{xy}f_{yx} = 0 \quad (2)$$

The first corrugation function to examine is given by:

$$f(x,y) = (\cos(x) + 2) \cdot (\cos(y) + 2) \quad (3)$$

Shown in figure 1 is: in part a) a 3-dimensional view on the surface unit cell; part b) shows the scattering profile at  $z=\infty$ ; in part c) the contour representation of the Hessian of this function has been plotted, and the last section (d) shows the corresponding caustics. In this case the Hessian looks like a difficult quadratic equation:

$$H[f(x,y)] = \cos(x)\cos(y)(\cos(x) + 2)(\cos(y) + 2) - \sin^2(x)\sin^2(y) \quad (4)$$

As is shown in figure 1c the equation  $H[f(x,y)] = 0$  defines two non-overlapping curves in the unit cell. Both curves give rise to a (non-overlapping) caustic, which has been plotted in figure 1d. Those caustics are examples of the catastrophes of lowest order, namely the fold and the cusp catastrophe. The outer struc-

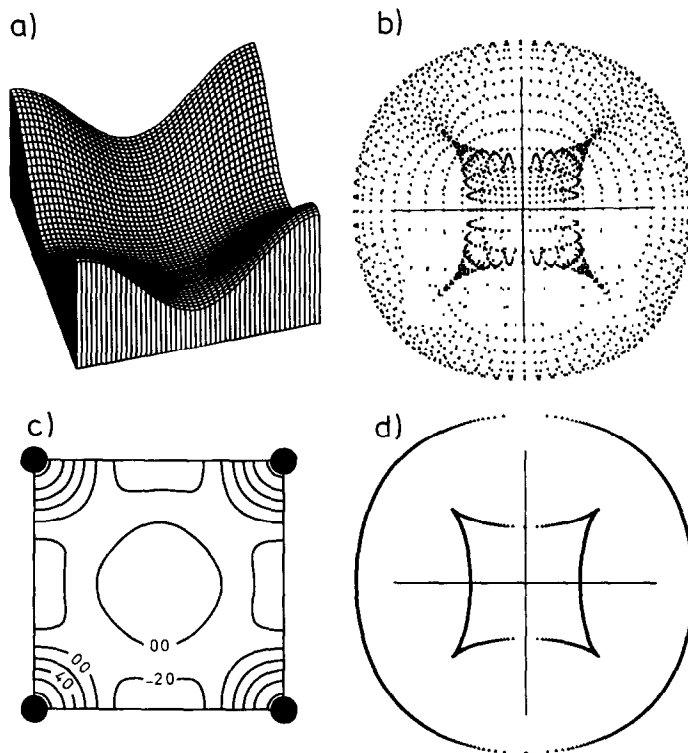


Fig. 1. Reflection from the corrugated hard wall  $f(x,y) = 0.05(\cos(x) + 2)(\cos(y) + 2)$ ; a) hard wall unit cell, b) scattering profile at infinity, c) Hessian contour plot, d) caustics corresponding to  $H=0$  curves.

ture in the scattering profile, let us call it the rainbow line following M. Berry [4], is a curved fold projection and originates from the curve round the atoms at the corners of the square unit mesh. The inner structure is a projection of four cusp catastrophes. Those cusps are due to scattering from the Hessian's zero-contour in the middle of the unit cell. Apparently there is no significant difference between those  $H=0$  curves. Being a mathematician one would proceed to calculate the generic functions of the fold and cusp catastrophe out of this example. But we will try to indicate the nature of the structures using physical arguments.

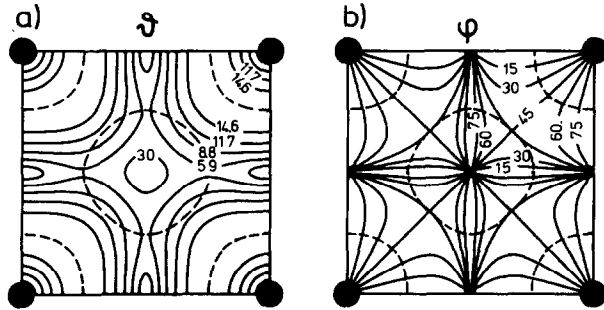


Fig. 2. Contour plots for the polar angle  $\theta$  (a) and for the azimuthal angle  $\phi$  (b), corresponding to reflection of figure 1 (the dotted lines represent the  $H=0$  curves).

To clarify our arguments contour representations of the two scattering angles involved in the process are shown in figure 2 as a function of the 2-dimensional impact parameter. In those plots the dotted lines represent the zero-contours of the Hessian of this surface. The information in such a contour representation is that a particle impinging on the surface at a certain point  $(x,y)$  will scatter off at an angle which can be read with the help of the contours. And so it can be noticed directly that the curve responsible for the rainbow line is situated on a flat region in the  $\theta$  contour plot. This means that the first derivatives of  $\theta$  to  $x$  and  $y$  are zero, which is indeed indicated by the name rainbow. In the  $\phi$  plot this curve lies in a region where the azimuthal angle changes almost constantly perpendicular to this curve. This gives rise to the folded structure called the rainbow line, which is almost independent of  $\phi$ .

On the contrary the effect of scattering along the second curve is not easily reflected in the contour plots of figure 2. Looking to the  $\theta$  plot it is obvious that along this curve nothing peculiar will happen. The polar angle will change from a minimum, through a maximum and back to the same minimum when the impact parameter walks along the curve. The minima lie on the  $x$  and  $y$  axes, while the maxima can be found on the diagonals of the square unit cell.  $\phi$  goes from 0 to 90 degrees, while no extrema is reached in between. The only remarkable fact is that again at the impact parameter where the  $H=0$  curve crosses the diagonal a very broad saddle point is present. The impact parameter in question is exactly the top of the saddle point. So scattering from this parameter will end up in a maximum in  $\theta$  and scattering around this point will be focussed into the  $\phi=45^\circ$  direction. This is the reason why a cusp catastrophe appears in the scattering profile.

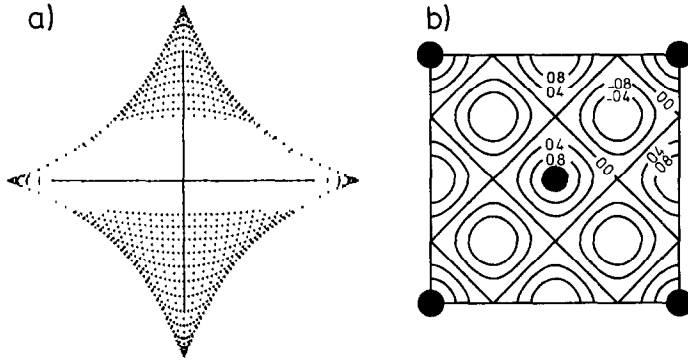


Fig. 3. Reflection from the corrugated hard wall  $f(x,y) = 0.6 \{ \cos(x) \cdot \cos(y) + 2 \}$ ; a) scattering profile at infinity, b) Hessian contour plot. (Note the atom in the middle of the unit cell.)

The second hard corrugated surface discussed in this paper is described by:

$$f(x,y) = \cos(x) \cdot \cos(y) + 2 \quad (5)$$

Because of the high symmetry in this corrugation, its Hessian is very simple:

$$H[f(x,y)] = \cos^2(x) - \sin^2(y) \quad (6)$$

In figure 3a the scattering profile has been plotted and in 3b the contour representation of the Hessian of this function. Here it can be seen that the two  $H=0$  curves from figure 1c have been changed into two squares, which are essentially the same, so that only one caustic is observed in the profile. Although this example looks much easier to handle, catastrophe theory tells that this is not the case. The hypersurface, constructed by the envelope of the trajectories of the particles after reflection, is degenerated as a consequence of the high symmetry of the surface. Breaking this symmetry is a rigorous condition to see one of the elementary catastrophes reflected in the scattering profile [4]. A calculation with a small, symmetry-breaking perturbation has been made and the result is plotted in figure 4. Immediately the hyperbolic umbilic catastrophe is recognized. This is fully equivalent to the results obtained by M. Berry using Kirchoff's approximation method [4].

To show that in this classical scattering model it is possible to predict the cusped structure without using the catastrophe theory, an expansion of  $g(\theta,\phi)=0$

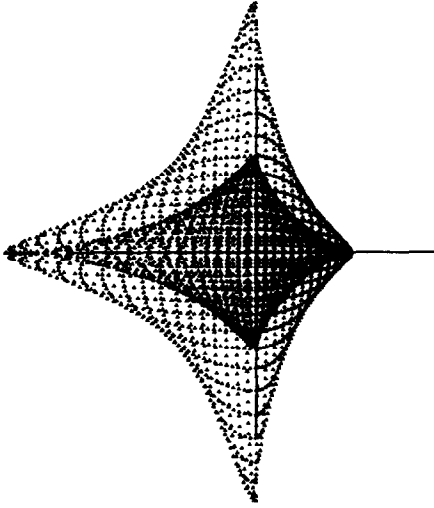


Fig. 4. Scattering profile at infinity of reflection from the perturbed hard wall  $f(x,y) = 0.6 \{ \cos(x) \cdot \cos(y) + 2 + \varepsilon \cdot (\cos(x) + \cos(y)) \}$ ,  $\varepsilon = 0.2$ .

round  $\phi = 0^\circ$  and  $\theta = \theta_{\text{rainbow}}$  is made. Substituting eq. (5) into the mapping for  $\theta$  and  $\phi$  (eq. (1a) and (1b)) and using goniometrical formulas one obtains:

$$g(\theta, \phi) = \cos(\theta) -$$

$$\frac{\pm \tan(\phi)}{\tan^2(\phi) \pm \tan(\phi) + 1} = 0 \quad (7)$$

Here the different signs are due to square roots in the equation  $H=0$  (see eq. (6)). For  $\phi \rightarrow 0^\circ$  the expansion becomes:

$$\cos(\theta) = \pm s - s^2 + 0(s^3), \quad s = \tan(\phi) \rightarrow 0 \quad (8)$$

So in first order the local behaviour of  $\partial\theta/\partial\phi$  is not univalent. This proves that the scattering profile contains a continuous but non-differentiable point at  $\phi = 0^\circ$ , like a mirror image in the  $\phi = 0^\circ$ -axis. This is equivalent with the projection of the cusp catastrophe.

#### SCATTERING FROM HARD SPHERES

To get an idea of the effect of double collisions a calculation of reflection from overlapping hard and massive spheres has been performed. To compare the results with our realistic simulation the spheres were placed on the positions of the W(110) surface atoms in a diamond-shaped unit cell. This W(110) unit cell is shown in the inset of figure 5, where the scattering profile for spheres with a radius of  $3 \text{ \AA}$  is given. In general the rainbow line originates from a curve around a crystal atom. Looking to scattering from this curve around atom 1 (see inset figure 5) shows that blocking will appear on the short axis (y-axis,  $\phi = 90^\circ$ ), due to the short distance to atom 3. Decreasing  $\phi$  will reduce this blocking so that a channeling direction at  $\phi = 70^\circ$  is generated. For  $70^\circ < \phi < 10^\circ$  blocking by atom 4 will occur. But now coming to the long axis (x-axis,  $\phi = 0^\circ$ ) no

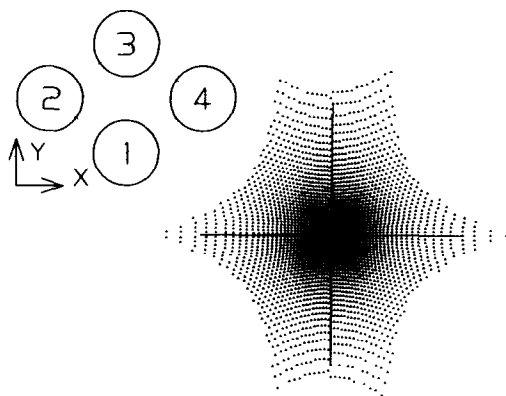


Fig. 5. Scattering profile at infinity of reflection from overlapping hard spheres with radii 3 Å and positioned in a W(110) unit cell.

blocking will be present anymore. The projectiles scattered off e.g. from atom 2 will be focussed into the  $\phi = 0^\circ$  direction by the atoms 1 and 3 on the short axis, while these atoms simultaneously shadow off atom 4. So also for  $\phi = 0^\circ$  a channeling direction is observed.

#### REALISTIC SIMULATION OF 35 eV K-SCATTERING ON W(110)

The simulations performed to fit a model potential and to understand our scattering data of 35 eV K-ions on W(110) will be extensively described elsewhere [2]. Here only the result of the classical trajectory calculation will be discussed. This result will be presented as a 3-dimensional hypersurface in  $(x, y, v')$ -space, where  $v'$  is the final velocity of the  $K^+$ . So this should be considered as a measurement performed with an imaginary spherical detector with velocity resolution, which is positioned with the surface in its centre and has a large radius like a LEED screen. In figure 6 three projections of this hypersurface are plotted: upon the  $xy$ -plane, the  $xv'$ -plane and the  $yv'$ -plane. We want to emphasize the difference between this simulation, including energy exchange, and the hard wall calculations, where the projectiles do not lose energy. Nevertheless, it is meaningful to compare the  $xy$ -plane projection of figure 6 to the former results. This follows from e.g. Li-scattering on W, which lets the hypersurface shrink into a thick layer of particles. It also can be seen when taking into account energy losses in a hard wall calculation, which will result in stretching of the flat layer of particles into a 3-dimensional hypersurface,

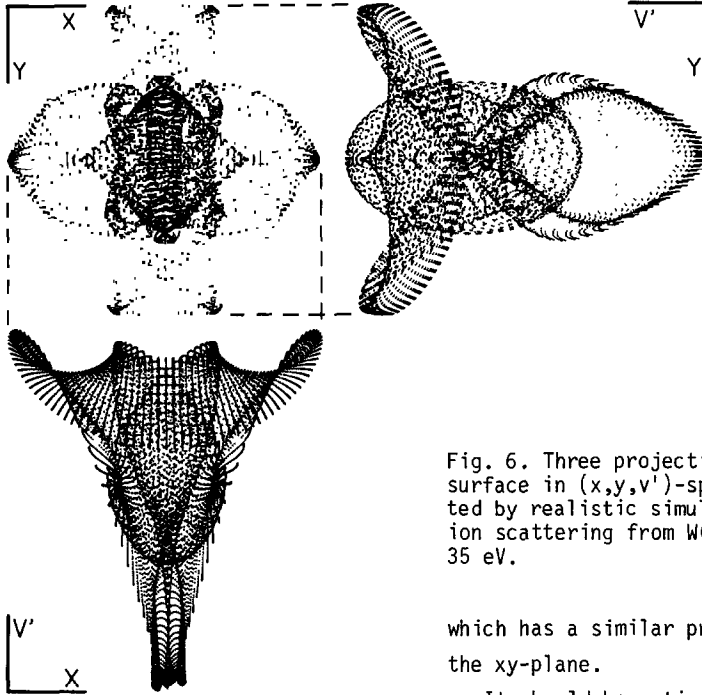


Fig. 6. Three projections of hypersurface in  $(x, y, v')$ -space, generated by realistic simulation for K-ion scattering from W(110) at 35 eV.

which has a similar projection on the  $xy$ -plane.

It should be noticed that projecting the hypersurface onto the  $xy$ -plane the information in energy, which has proven to be very valuable in the initial understanding of the scattering mechanism [1,2], will get lost. But one should bear

in mind that in this particular representation of our realistic simulation a complete view on the azimuthal dependence of the scattering is gained.

The projection to the  $xy$ -plane is the integral over all scattered projectiles seen by the spherical detector. Let us concentrate on that projection. Besides many structures in this picture, the rainbow line can be observed well. This line resembles that one observed in the hard sphere calculation: the blocking in  $\phi = 90^\circ$  and the channeling in  $\phi = 0^\circ$  and  $70^\circ$  direction. It should be remarked that in this simulation a simultaneous interaction with several crystal atoms takes place and it is impossible to speak about single or double collisions. At  $\phi = 70^\circ$  a double folded structure can be recognized. Clearly the two folded structures in the  $\phi = 0^\circ$  and  $90^\circ$  directions at the rainbow line have a different status. The latter is just a folded surface, but the first one is a projection of a fol-



ded saddle point as can be seen at the projection onto the  $xv'$ -plane. The structure in the middle of the hypersurface is caused by scattering from the hollow site in the unit cell, where energy transfer has been shown to be important. The structure contains several rainbowlike features [1,2], and is difficult to unravel, but looking to a video tape of sections with fixed  $v'$  gives an impression which is based on some elementary catastrophe plots. It is possible to recognize fold, cusp and swallow-tail catastrophes.

#### CONCLUSIONS

Simple hard wall scattering simulations can teach us about the use of catastrophe theory to analyze realistic scattering data. Further efforts will be made to describe our data in terms of elementary catastrophes and eventually this type of analysis could be used as a powerful tool to analyze characteristic features of the gas-surface interaction potential.

The authors like to thank Dr. N.M. Temme and Drs. G.F. Pouwels for helpful mathematical discussions and remarks, and Prof.dr. J. Los for his stimulating and continuous interest in this work. This work is sponsored by FOM (Stichting voor Fundamenteel Onderzoek der Materie) with financial support from ZWO (Nederlandse Organisatie voor Zuiver-Wetenschappelijk Onderzoek).

#### REFERENCES

- 1 A. Tenner, K. Gillen, T. Horn, J. Los and A. Kleyn, 1984, Phys.Rev.Letters 52, p.2183.
- 2 A. Tenner, R. Saxon, K. Gillen, D. Harrison, T. Horn and A. Kleyn, to be published.
- 3 T. Poston and I. Stewart, 1978, Catastrophe Theory and its Applications (Pitman).
- 4 M. Berry, 1975, J.Phys.A: Math.Gen., vol. 8, no. 4, p.566.